ACS APPLIED MATERIALS & INTERFACES

Research Article

www.acsami.org

A Surface with Superoleophilic-to-Superoleophobic Wettability Gradient

Guangyu Zhang, Xin Zhang, Meng Li, and Zhaohui Su*

State Key Laboratory of Polymer Physics and Chemistry, Changchun Institute of Applied Chemistry, Chinese Academy of Sciences, Changchun 130022, People's Republic of China

Supporting Information

ABSTRACT: A strategy combining polyelectrolyte multilayer (PEM) deposition and counterion exchange was developed to fabricate wettability gradient surfaces on rough aluminum with wetting characters continuously varied from superoleophilic to superoleophobic. Counterion exchange kinetics was adopted as a means to tailor the surface chemical composition spatially, with the gradient ultimately reflecting position-dependent immersion time during the dipping of substrate in salt solution. Wettability depended on the identity and concentration of the counterion in the outermost PEM layer. Gradients could be erased and rewritten through the exchange of counterions, and the gradient's wetting character was evaluated by measuring both water and oil contact angles. The surface chemical composition gradient was further investigated by X-ray photoelectron spectroscopy.

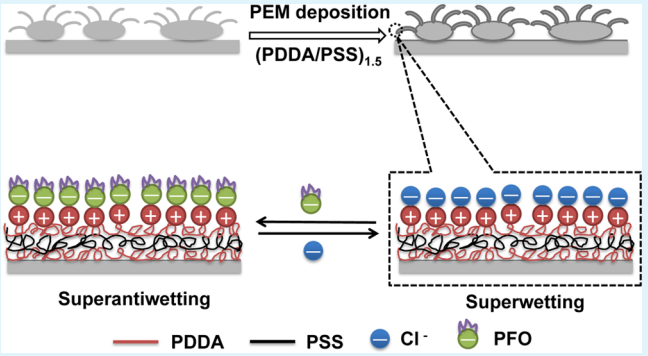

KEYWORDS: *polyelectrolyte multilayers, counterion, gradient, superoleophobicity, surface, wettability*

INTRODUCTION

An important characteristic of solid surfaces, wettability is governed by both surface chemical composition and surface morphology.[1−3] In the past decade, superhydrophobic surfaces, those with a water contact angle (WCA) larger than 150° and low contact angle hysteresis, and superhydrophilic surfaces, those with a WCA smaller than 5°, have been extensively studied for applications as various as antifogging, self-cleaning, anticorrosion, and water harvesting. Generally, superhydrophobic surfaces are prepared from hydrophobic surfaces by tailoring surface topography, whereas superhydrophilic surfaces are realized by imposing a 2D or 3D capillary effect on hydrophilic surfaces.[4] Recently, superoleophobic surfaces, those with an oil contact angle (OCA) higher than 150° and low contact angle hysteresis, and superoleophilic surfaces, those with an OCA lower than 5°, have garnered fundamental and practical interest. Tsujii and co-workers demonstrated that the combination of a fractal rough surface topography and a low surface energy (e.g., trifluoromethyl coating) is essential to superoleophobicity;[5] Jiang and co-workers demonstrated superoleophobicity on micro/nano hierarchically textured surfaces of a fluorine-containing polymer;[6] and Tuteja and co-workers showed that reentrant curvature has a crucial role in surface superoleophobicity.[7] Further, superoleophilic and superhydrophobic surfaces have been joined in one mesh for oil/water separation.[3,8] Beyond these examples, wettability gradient surfaces are often of interest in the contexts of cell motility, biomolecular interactions, and microfluidics.[9−11]

Several preparation techniques for gradient surfaces have been described, including chemical vapor deposition, corona discharge,[12] and gradual immersion,[10,13] leading to different kinds of gradients, mainly those in chemical composition[13−15] and in surface topology.[9,16] Together, composition and topology determine the macroscopic surface energy, which controls wettability.[3,4] Therefore, almost all surface gradients display gradients in wettability.[14] Wettability gradient surfaces have traditionally been characterized with water as the probe liquid. For instance, Whitesides and co-workers demonstrated that water drops move across a surface that exhibits a spatial variation from hydrophilic to hydrophobic.[17] In addition, Zhang and co-workers fabricated gradient surfaces with extreme variations in wetting, from superhydrophobic to superhydrophilic.[10] In a previous work,[13] we fabricated a tunable and rewritable wettability gradient on a gold substrate, with wetting also altered from superhydrophobic to superhydrophilic. However, to our knowledge, oily wettability gradient surfaces, those displaying properties from superoleophilic to superoleophobic, have not been reported. Such surfaces potentially can be applied in fluid transport, nanotribology, and lab-on-chip technologies.

Over the past decades, the layer-by-layer (LbL) deposition technique,[18] which creates a thin polyelectrolyte multilayer (PEM) film via the dipping of a substrate alternately into

Received: October 22, 2013
Accepted: January 3, 2014
Published: January 13, 2014

   dx.doi.org/10.1021/am404681y | ACS Appl. Mater. Interfaces 2014, 6, 1729−1733

positive and negative polyelectrolyte solutions, has become a mature approach to surface modification.[19,20] The LbL technique can be applied to just about any kind of solid substrate, even nonadhesive hydrophobic poly(tetrafluoroethylene) (PTFE), without concern for substrate shape or surface topology. The counterions coordinated with the outermost (i.e., last deposited) polyelectrolyte influence the surface energy and strongly affect the apparent contact angle. Counterion exchange, driven by the alteration of identity or concentration for counterion in an overlying solution, permits straightforward manipulation of surface chemical composition, and, thereby, surface free energy.[13] Herein, we report a facile LbL strategy, involving the PEM deposition and subsequent counterion exchange with perfluorooctanoate (PFO) anions, to create gradient surfaces on rough aluminum with wetting properties continuously varied from superoleophilic to superoleophobic.

EXPERIMENTAL SECTION

Materials. Poly(diallyldimethylammonium chloride) (PDDA, M_w = 200−350k), and poly(sodium 4-styrene sulfonate) (PSS, M_w = 70k) were both purchased from Sigma-Aldrich. Sodium perfluorooctanoate [$CF_3(CF_2)_6COONa$, 97+%] was purchased from J&K Scientific, and hexadecane, diiodomethane, sodium chloride, ethanol, chloroform, acetone, and perchloric acid were all purchased from Aladdin Chemical Reagent Co. Ltd. (Shanghai, China) and used without additional purification. An aluminum plate of 0.5 mm in thickness was purchased from a local metal supplier and cut into 70 × 15 mm^2 substrate pieces. Water for rinsing, or to act as solvent, was of Millipore quality (resistivity 18.2 MΩ·cm).

Micro/Nano Structured Surface. The cut aluminum pieces were ultrasonically cleaned for 2 min each in deionized water, ethanol, chloroform, and acetone to remove impurities. Afterward, the cleaned and dry aluminum substrate was electrochemically polished to high smoothness in a perchloric acid/ethanol solution (25 mL of $HClO_4$, 4 mL of H_2O, 290 mL of C_2H_5OH), with the 60 V treatment extending to 3 min, and then rinsed with deionized water and dried with nitrogen. A micro/nano hierarchical surface was produced on the smoothed substrate by a literature procedure.[21] In this procedure, the substrate is first etched at room temperature in 2.5 M HCl and then is immersed for 20 min in boiling deionized water and finally dried with nitrogen.

PEM Deposition and Counterion Exchange. A $(PDDA/PSS)_{1.5}$ PEM film was applied to the rough aluminum substrate following a literature procedure[13] that alternately dips the substrate for 15 min into PDDA (1.0 mg/mL, with 1.0 M NaCl present) and PSS (1.0 mg/mL, with 1.0 M NaCl present) aqueous solutions, and then into PDDA again, with a water rinse included after each dipping. Counterion exchange of the PEM surface was realized by immersing a PEM-coated substrate in the requisite anion aqueous solution before another rinse with water and drying with nitrogen. To fabricate wettability gradient surfaces for water, diiodomethane, and hexadecane, a relatively uncomplicated strategy was adopted: a vertically oriented PEM-coated substrate was dipped at ca. 1 mm/s into PFO aqueous solutions. Three PFO concentrations were selected for the dipping, 0.05 mM, 0.15 mM, and 0.1 M. After the constant speed dipping, the substrate was rapidly withdrawn from the PFO solution before rinsing with water and drying with nitrogen.

A surface gradient was erased by immersing the substrate in a NaCl aqueous solution (1 M) for 10 min and rewritten by reimmersing the substrate in a PFO solution of appropriate concentration. This process can be repeated.

Characterization. A field emission scanning electron microscope (FESEM, FEI XL30) provided images of morphology for the smooth, roughened, and PEM-deposited surfaces, and XPS data for these surfaces were obtained from a Thermo-electron ESCALAB 250 spectrometer with a focused monochromatic Al X-ray source (1486.6 eV). The analyzer's pass energy was set to 50 eV to record survey spectra and 20 eV to record high-resolution spectra. A $(PDDA/PSS)_{1.5}$ PEM film was assembled on a clean silicon wafer, and its thickness was measured using a UVISEL ER ellipsometer. Surface wettability was evaluated with a ramé-hart 200-F1 goniometer at ambient temperature for the following probe liquids (and droplet volumes): water (3 μL), diiodomethane (3 μL), and hexadecane (2 μL). Each contact angle reported here is an average value of at least five independent measurements.

RESULTS AND DISCUSSION

A rough starting surface topology is needed to prepare a superwetting or superantiwetting surface.[13] Here, oppositely charged polyelectrolytes, PDDA and PSS, were deposited on rough aluminum to form a PEM with PDDA as the capping layer. The counterion to this capping layer was then exchanged by exposure to a solution of PFO, which dramatically modifies the surface energy. In this way, a surface with a tunable, erasable, and rewritable continuous wettability gradient was fabricated. Scheme 1 illustrates the overall procedure.

Scheme 1. Schematic Depiction of the Procedure by Which PEM Deposition and Counterion Exchange Was Achieved on a Micro/Nano Hierarchical Aluminum Surface

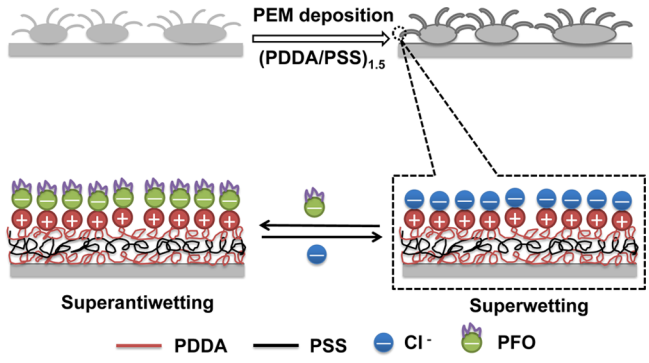

Rough aluminum was chosen as an illustrative substrate for its preparation simplicity and chemical robustness. As shown in Figure 1a, the electrochemically polished aluminum surface was smooth to the micrometer scale. Etching to create roughness was accomplished by exposure to 2.5 M HCl, followed by boiling in water. Figure 1b−d displays typical FESEM images of the roughened surface at increasing magnification. Micrometer-scale granular, or star-shaped, asperities are seen to be accompanied by ca. 200 nm level irregular flaking, the latter attributed to the boiling water treatment.[22,23] Similar surface morphology was observed when the boiling water treatment was extended from 20 to 30 min (Supporting Information, Figure S1). During the boiling treatment, crystalline boehmite, AlO(OH),[23] helpful for the subsequent PEM deposition, formed. The type of micro/nano hierarchical surface morphology seen here is known to enhance wetting properties greatly, as reported many times before and offered in explanation for the "lotus leaf" effect.[24]

In aqueous solution, the many aluminol groups on the roughened aluminum surface bestowed on this surface a slightly negative charge density that facilitated the adsorption of positively charged PDDA. Even a thin (ca. 3.3 nm thickness, Supporting Information, Figure S2) $(PDDA/PSS)_{1.5}$ PEM afforded significant antiwetting properties in air to the roughened surface.[21] Because of its thinness, the PEM hardly

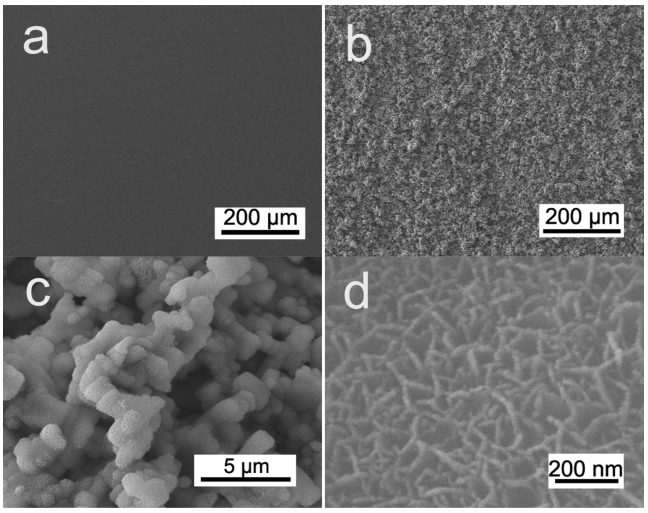

Figure 1. FESEM images of smoothed and textured aluminum surfaces: (a) smooth starting surface, (b) rough etched surface at low magnification, (c) rough etched surface at higher magnification, (d) rough etched surface at even higher magnification showing nanofeatures on a microflake.

altered the underlying surface roughness, a characteristic crucial to the desired wettability attributes.

With Cl^- remaining the counterion coordinated to the outermost positive polyelectrolyte, the treated surface is superoleophilic AND superhydrophilic, as shown on the leftmost side of the row of images in Figure 2, which display contact angles < 5° for both water and oily probe liquids. These characters reflect the 3D capillary effect:[4] probe liquids penetrated the cavities and so the wetting domain was in the Wenzel state, with the apparent contact angle smaller than that for the flat surface (Supporting Information, Figure S3).[25] However, after Cl^- anions were replaced by PFO anions, the surface became superoleophobic AND superhydrophobic, with a static contact angle of ca. 159 ± 3° (water), 156 ± 3° (diiodomethane), and 154 ± 4° (*n*-hexadecane). Droplets of any of these liquids did not rest on the surface if the substrate was tilted from the horizontal by >5°, a test result implying minimal contact angle hysteresis. These properties are consistent with wetting in the Cassie–Baxter state.[26] High static contact angle and low contact angle hysteresis emerge from a coupling between a low surface energy surface composition and a hierarchical surface topography, which, together, trap air in the cavities between solid and liquid. While in the literature the low surface energy materials employed are mostly fluoropolymers[3,27,28] and silicones,[29−31] in the present study, low surface energy (and hence superantiwetting properties) was achieved using typical polyelectrolytes, with a perfluoro anion that coordinates with the polycation. The surface energy can be readily tuned by changing the identity and content of the anion,[13,19] making the approach extremely versatile.

When surface topologies are identical, wettability is determined by chemical composition. A gradient in counterion species can thus spatially vary the wettability of a PEM-coated surface. Here, a continuous gradient of PFO was created under the control of ion-exchange kinetics, which, in turn, was under the control of immersion time in PFO solution (Supporting Information, Figure S4). When the PEM-deposited substrate was slowly dipped into PFO solution with the PEM film held perpendicular to the solution–air interface, immersion time increased linearly in inverse proportion to surface vertical position; with the steady dipping velocity of ca. 1 mm/s, this time varied from ca. 5 to 55 s along the 7 cm long surface. As displayed across Figure 2, these time differences made the contact angle continuously increase from <5° to >150° for both water (Figure 2a) and oil (Figure 2b,c). For PFO bath concentrations of 0.05 mM, 0.15 mM, and 0.1 M, the wetting of water, diiodomethane, and hexadecane all smoothly shifted from superwetting to superantiwetting.

The replacement of Cl^- by PFO was further characterized by XPS, applied at different positions along the gradient. Illustrating with the water wettability gradient surface (Figure 1a), the PEM-coated substrate was cut into seven equal pieces along the gradient, the immersion time rising from 0 to 55 s, and each piece was examined by XPS, with results given in Figure 3. With increased immersion time, Figure 3a shows that the Cl 2p peak (at 196.7 eV) weakens gradually. Oppositely, Figure 3b reveals that the F 1s peak (at 688.6 eV) significantly strengthens. Concurrently, Figure 3c shows that the S 2p peak (at 167.1 eV) stays constant, an expected result since this peak captures only the invariant sulfonate groups of PSS. Combining panels b and c in Figure 3, Figure 3d provides the fluorine-to-sulfur (F/S) ratio, the most decisive evidence for the composition gradient. Interestingly, the composition gradient

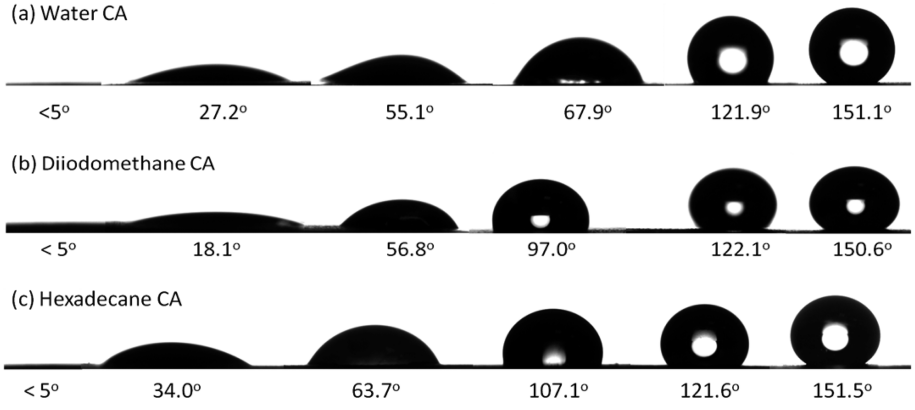

Figure 2. Optical images of probe liquid droplets on wettability gradient surfaces, with contact angle given below each image: (a) Water, (b) Oil (diiodomethane), (c) Oil (*n*-hexadecane). Each sequence combines six droplet images because the goniometer view is too narrow to capture the entire gradient length. From left to right, PFO increasingly replaced Cl^-.

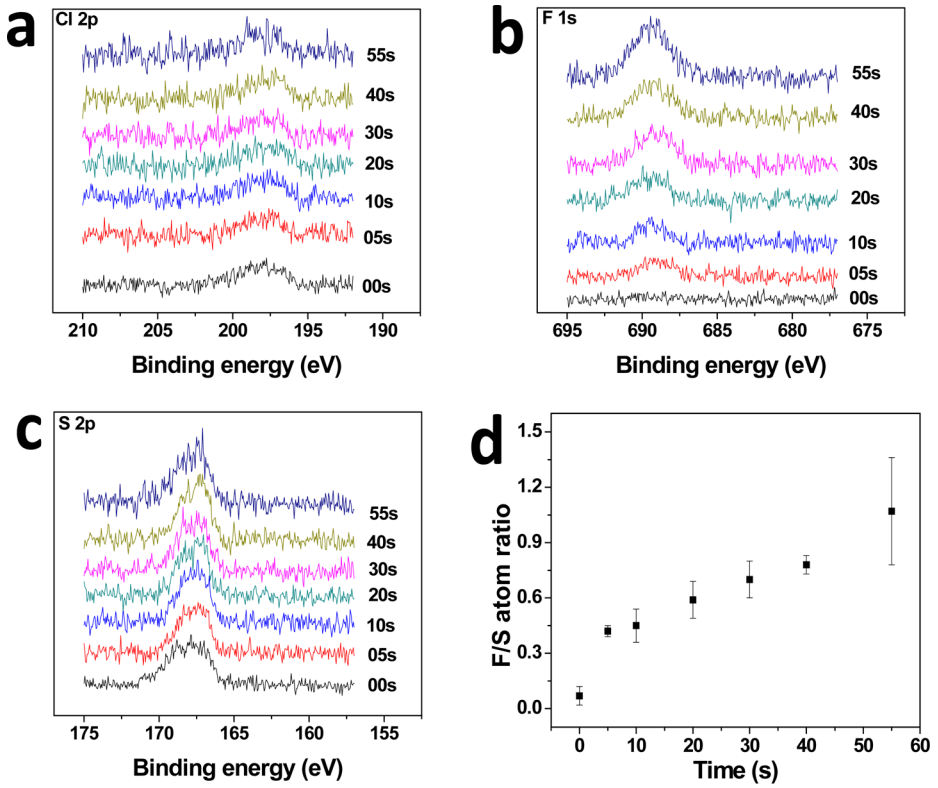

Figure 3. XPS spectra at seven positions along the water wettability gradient of (a) Cl 2p, (b) F 1s, and (c) S 2p regions. (d) F/S atomic ratio.

was not linear; without experiments at different dipping speeds, this trend should not be overemphasized. However, linearity would not be expected unless the PFO uptake was linear in immersion time, a trend not expected for diffusion-controlled ion exchange kinetics.

With ion exchange in the outermost PEM layer entirely reversible,[13] a surface wettability gradient can be erased by immersion in 1 M NaCl and then reestablished by controlled dipping back into PFO. Figure 4 shows five cycles of reversible

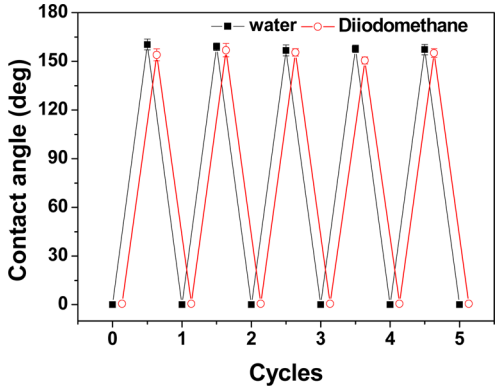

Figure 4. Superwetting-to-superantiwetting transition repeated five times by the alternating ion exchange of Cl^- and PFO.

superwetting-to-superantiwetting transition achieved at one surface position, each erasure and rewriting confirmed by both water and diiodomethane contact angle. A different wettability gradient can also be written on an erased surface, as verified by reversing the direction of a wettability gradient.

Switchable wetting and switchable wettability gradients have been reported before.[10,13] However, to our knowledge, fully and repeatedly reversed wettability gradients have not been demonstrated. To test whether the reported gradients have these properties, a PEM-coated substrate was cut into seven identical pieces, which were dipped into room-temperature 0.05 mM PFO for periods of 0−55 s. As shown in Figure 5, each of

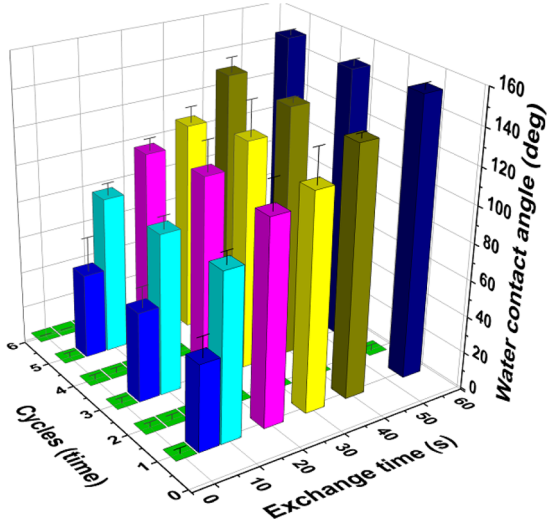

Figure 5. Water contact angles erased and rewritten three times for different periods of immersion in 0.05 mM PFO.

these surfaces was first characterized by water contact angle, erased in 1 M NaCl for 10 min, and rewritten in 0.05 mM PFO for the original period. This wetting cycle exercise was repeated three times, with results as given in Figure 5. Contact angles after each cycle were essentially the same, demonstrating the desired properties.

dx.doi.org/10.1021/am404681y | ACS Appl. Mater. Interfaces 2014, 6, 1729−1733

CONCLUSIONS

Surfaces with spatial wettability gradients spanning from superoleophilic and superhydrophilic to superoleophobic and superhydrophobic were fabricated on rough aluminum substrates via a two-step process of PEM deposition and counterion exchange. In a manner dependent on the period of ion exchange, the latter step replaced Cl^- with PFO in the PEM's outermost layer. This period could be varied across a surface by controlled rate dipping. The good effectiveness of this new surface modification strategy was tested by measuring the contact angle gradient (for water and oil) and the surface composition gradient (by XPS). Most importantly, wetting could be reversibly and repeatedly altered from one state to another everywhere along a gradient. The simple and versatile procedure described in this contribution should be easy to implement in technologies requiring robust wetting gradients.

ASSOCIATED CONTENT

Supporting Information

More characterization data and counterion exchange kinetics. This material is available free of charge via the Internet at http://pubs.acs.org.

AUTHOR INFORMATION

Corresponding Author

*E-mail: zhsu@ciac.ac.cn. Phone: (+86)431-85262854. Fax: (+86)431-85262126.

Notes

The authors declare no competing financial interest.

ACKNOWLEDGMENTS

This work is supported by the National Natural Science Foundation of China (21174145). Z.S. thanks the NSFC Fund for Creative Research Groups (50921062) for support.

REFERENCES

(1) Chen, W.; Fadeev, A. Y.; Hsieh, M. C.; Öner, D.; Youngblood, J.; McCarthy, T. J. *Langmuir* **1999**, *15*, 3395−3399.
(2) Öner, D.; McCarthy, T. J. *Langmuir* **2000**, *16*, 7777−7782.
(3) Feng, L.; Zhang, Z.; Mai, Z.; Ma, Y.; Liu, B.; Jiang, L.; Zhu, D. *Angew. Chem., Int. Ed.* **2004**, *43*, 2012−2014.
(4) Sun, T. L.; Wang, G. J.; Feng, L.; Liu, B. Q.; Ma, Y. M.; Jiang, L.; Zhu, D. B. *Angew. Chem., Int. Ed.* **2004**, *43*, 357−360.
(5) Tsujii, K.; Yamamoto, T.; Onda, T.; Shibuichi, S. *Angew. Chem., Int. Ed.* **1997**, *36*, 1011−1012.
(6) Xie, Q.; Xu, J.; Feng, L.; Jiang, L.; Tang, W.; Luo, X.; Han, C. C. *Adv. Mater.* **2004**, *16*, 302−305.
(7) Tuteja, A.; Choi, W.; Ma, M. L.; Mabry, J. M.; Mazzella, S. A.; Rutledge, G. C.; McKinley, G. H.; Cohen, R. E. *Science* **2007**, *318*, 1618−1622.
(8) Wang, S. T.; Song, Y. L.; Jiang, L. *Nanotechnology* **2007**, *18*, 1−5.
(9) Zhang, J.; Xue, L.; Han, Y. *Langmuir* **2004**, *21*, 5−8.
(10) Yu, X.; Wang, Z.; Jiang, Y.; Zhang, X. *Langmuir* **2006**, *22*, 4483−4486.
(11) Neuhaus, S.; Padeste, C.; Spencer, N. D. *Langmuir* **2011**, *27*, 6855−6861.
(12) Jeong, B. J.; Lee, J. H.; Lee, H. B. *J. Colloid Interface Sci.* **1996**, *178*, 757−763.
(13) Wang, L.; Peng, B.; Su, Z. *Langmuir* **2010**, *26*, 12203−12208.
(14) Liedberg, B.; Tengvall, P. *Langmuir* **1995**, *11*, 3821−3827.
(15) Morgenthaler, S.; Lee, S.; Zürcher, S.; Spencer, N. D. *Langmuir* **2003**, *19*, 10459−10462.
(16) Zhang, J. L.; Han, Y. C. *Langmuir* **2008**, *24*, 796−801.
(17) Chaudhury, M. K.; Whitesides, G. M. *Science* **1992**, *256*, 1539−1541.
(18) Decher, G. *Science* **1997**, *277*, 1232−1237.
(19) Wang, L.; Lin, Y.; Peng, B.; Su, Z. *Chem. Commun.* **2008**, 5972−5974.
(20) Wang, L.; Lin, Y.; Su, Z. *Soft Matter* **2009**, *5*, 2072.
(21) Yang, J.; Zhang, Z.; Men, X.; Xu, X.; Zhu, X.; Zhou, X.; Xue, Q. *J. Colloid Interface Sci.* **2012**, *366*, 191−195.
(22) Tadanaga, K.; Katata, N.; Minami, T. *J. Am. Ceram. Soc.* **1997**, *80*, 3213−3216.
(23) Hozumi, A.; Kim, B.; McCarthy, T. J. *Langmuir* **2009**, *25*, 6834−6840.
(24) Sun, M.; Luo, C.; Xu, L.; Ji, H.; Ouyang, Q.; Yu, D.; Chen, Y. *Langmuir* **2005**, *21*, 8978−8981.
(25) Wenzel, R. N. *Ind. Eng. Chem.* **1936**, *28*, 988−994.
(26) Cassie, A. B. D.; Baxter, S. *Trans. Faraday Soc.* **1944**, *40*, 546−551.
(27) Zhai, L.; Cebeci, F. Ç.; Cohen, R. E.; Rubner, M. F. *Nano Lett.* **2004**, *4*, 1349−1353.
(28) Ou, J.; Hu, W.; Xue, M.; Wang, F.; Li, W. *ACS Appl. Mater. Interfaces* **2013**, *5*, 9867−9871.
(29) Jin, M. H.; Feng, X. J.; Xi, J. M.; Zhai, J.; Cho, K. W.; Feng, L.; Jiang, L. *Macromol. Rapid Commun.* **2005**, *26*, 1805−1809.
(30) Gao, L.; McCarthy, T. J. *J. Am. Chem. Soc.* **2006**, *128*, 9052−9053.
(31) Zhang, J.; Seeger, S. *Angew. Chem., Int. Ed.* **2011**, *50*, 6652−6656.